Kinetic identification of membrane transporters that assist P-gp mediated transport of digoxin and loperamide through a confluent monolayer of MDCKII-hMDR1 cells.

Poulomi Acharya, Michael P. O'Connor, Joseph W. Polli, Andrew Ayrton, Harma Ellens & Joe Bentz

Department of Bioscience & Biotechnology, Drexel University, Philadelphia, PA19104, USA (PA, MO and JB)

[2] Preclinical Drug Metabolism and Pharmacokinetics, GlaxoSmithKline, King of Prussia, PA, 19406. (PA and HE)

[3] Preclinical Drug Metabolism and Pharmacokinetics, GlaxoSmithKline, Research Triangle Park, NC 27709 (JWP)

[4] Preclinical Drug Metabolism and Pharmacokinetics, GlaxoSmithKline, Welwyn, England (AA)

Running Title: Kinetic identification of membrane transporters.

Address correspondence to:

Dr. Joe Bentz, Dept. of Bioscience & Biotechnology, Drexel University, 32nd& Chestnut Sts.,

Philadelphia, PA, 19104, Phone: 215-895-1513, email: bentzj@drexel.edu, FAX: 215-895-1273.

Text Pages: (3 to 28) total=26 pages

Figures: 4

Tables: 2

References: 40

Abstract word count: 232 (Max limit = 250)

Introduction word count: 678 (Max limit = 750)

Discussion word count: 1427 (Max limit = 1500)

Non-standard Abbreviations: P-gp, the P-glycoprotein product of the hMDR1 gene; A>B (or

B>A), transport across the confluent cell monolayer when the donor chamber is apical (or

basolateral) and the receiver chamber is basolateral (or apical).

Abstract

A robust screen for compound interaction with P-gp requires a cell line expressing P-gp and a

probe-substrate which is transported solely by P-gp and passive permeability. While this is

obvious, it is actually difficult to prove that a particular probe substrate interacts only with P-gp

in the chosen cell line. Using a confluent monolayer of hMDR1-MDCKII cells, we have

determined the elementary rate constants for the P-gp efflux of amprenavir, digoxin, loperamide,

and quinidine. For amprenavir and quinidine, transport was fitted with just P-gp and passive

permeability. For digoxin and loperamide, fitting required a basolateral transporter ($p<0.01$),

which was inhibited by the P-gp inhibitor GF120918. This means that when digoxin is used as a

probe-substrate and a compound is shown to inhibit digoxin flux, it could be that the inhibition

occurs at the basolateral transporter, rather than at P-gp. Digoxin B>A efflux also required an

apical importer ($p<0.05$). We propose that amprenavir and quinidine are robust probe-substrates

for assessing P-gp interactions using the MDCKII-hMDR1 confluent cell monolayer. Usage of

another cell line, e.g., LLC-hMDR1 or Caco-2, would require the same kinetic validation to

ensure the probe substrate only interacts with P-gp. Attempts to identify the additional digoxin

and loperamide transporters using a wide range of substrates/inhibitors of known epithelial

transporters (OCT, OAT, OATP, URAT or MRP) failed to inhibit the digoxin or loperamide

transport through their basolateral transporter.

Introduction

The importance of membrane transporters in the metabolism and disposition of drugs is well

recognized (Mizuno et al., 2003; Collett et al., 2005; Spears et al., 2005; Shitara et al., 2006;

Robertson and Rankin, 2006; Sekine et al., 2006). While it seems clear that membrane

transporters mediate the transcellular transport of compounds across epithelial and endothelial

barriers, it has proven challenging to identify which uptake and efflux transporters are involved

with a particular compound *in vivo* (Lau et al., 2006). Cell lines over-expressing individual

transporters have proven quite useful in this respect, both in identifying substrates as well as

inhibitors of the transporter in question.

The human multidrug resistance transporter P-glycoprotein, P-gp (Juliano and Ling, 1976), is the

product of the hMDR1 (ABCB1) gene, and is widely expressed in human epithelial tissue as a

protection against xenobiotics (Dean et. al., 2001). Polarized confluent cell monolayers over-

expressing P-gp have been used extensively as a model system to study P-gp transport

mechanisms and to assess the risk of P-gp-mediated drug-drug interactions (Tang et al., 2002;

Rautio et al., 2006; Korjamo et al., 2007; Bartholome et al., 2007).

Using the polarized MDCKII-hMDR1 confluent cell monolayer, which over-expresses human P-

gp in the apical plasma membrane, and a detailed mass action analysis of P-gp efflux kinetics,

we have been able to answer several fundamental questions about P-gp function (Tran et al.,

2005; Bentz et al, 2005, 2007; Acharya et al. 2006). With P-gp as the only transporter in the

kinetic model, we have found that amprenavir and quinidine were well fitted, while loperamide

showed more efflux than could be explained by just P-gp (Tran et al., 2005; Acharya et al.,

2006). Previous work had shown other transporters in model cell lines. Secretory transport of

rhodamine 123 across Caco-2 cell monolayers involves a basolateral uptake transporter in addition to P-gp (Troutman and Thacker, 2003). MDCKII wild-type cells and MDCKII cells over-expressing bcrp1 contain an apical influx transporter for the BCRP substrate mitoxantrone (Pan and Elmquist, 2007).

These observations led to (1) the speculation that there was another transporter involved for loperamide in the MDCKII-hMDR1 cells and (2) to the question of the extent to which other transporters in these cells might affect inhibition of a probe-substrate in screening for drug-drug interactions with P-gp. A "robust" probe-substrate for P-gp inhibition screening should be transported across the cell monolayer solely by P-gp and the passive permeability, which is measured in the presence of a potent P-gp inhibitor, like GF120918. In this case, the P-gp mediated efflux can be roughly estimated by the difference between the two curves, i.e. the total efflux(-GF120918)- the passive efflux (+GF120918). We say roughly since backflow, from receiver side to donor side, must be ignored (Tran et al., 2005).

If a probe-substrate also utilizes another transporter, then there are two possibilities. The first case is easy. If this new transporter is not inhibited by GF120918, then the +GF120918 efflux would contain both the contributions from the other transporter and from passive permeability. In this case, the difference between the two curves would still be due to P-gp alone. One just needs to be clear that "passive permeability" ,+GF120918, measurements can include transporters. The second case is the problem. If the novel transporter is inhibited by GF120918, then the "passive permeability", +GF120918, will underestimate the amount of probe-substrate actually reaching P-gp in the –GF120918 experiment. Then the difference between the curves yields an overestimate of the P-gp mediated efflux. Now, if a novel compound binds to and inhibits the other transporter, -GF120918, then less probe-substrate will reach P-gp, thus

reducing its efflux kinetics. Such a reduction would likely be misinterpreted as the novel compound being a P-gp inhibitor.

Here we have used our kinetic analysis to detect the presence of novel transporters of loperamide and digoxin in the basolateral membrane of this cell line, as well as a digoxin transporter in the apical membrane. Digoxin has been used as a probe-substrate with the MDCKII-hMDR1 confluent cell monolayers to screen novel compounds for P-gp inhibition (Rautio et al., 2006). A rigorous statistical analysis confirms the need for these additional transporters and thus supports our kinetic findings. For amprenavir and quinidine, only P-gp and passive efflux (-GF120918) is required to fit the data, suggesting that they are robust probe-substrates for this cell line.

Materials and Methods

Materials. Amprenavir and GF120918 were from GlaxoSmithKline Pharmaceuticals (USA), loperamide was from Sigma, and quinidine from Fisher Scientific. ^{3}H-loperamide (10 Ci/mmole) and ^{3}H-amprenavir (21 Ci/mmole) were custom synthesized by Amersham Pharmacia Biotech, England. ^{3}H-quinidine (20 Ci/mmole) was from ICN Biomedical, Inc. USA. Dulbecco's Modified Eagle Medium (DMEM) was from MediaTech, VWR. DMEM with 25 mM HEPES buffer, high glucose (4.5 g/L), L-Glutamine, FBS, pyridoxine hydrochloride, w/o sodium pyruvate, and with phenol red was from Gibco. The same medium without phenol red was used for transport experiments, denoted transport media. Transwell 12-well plates with polycarbonate inserts (0.4um pore size and 12 mm diameter) were obtained from Costar (Acton, MA). All compounds tested in Table 2 were from Sigma Chemical Co., St. Louis, MO.

Cell line and culture conditions. The Madin-Darby Canine Kidney II cell line that over-expresses human MDR1 (MDCKII-hMDR1) was purchased from the Netherlands Cancer Institute (Amsterdam, Netherlands). MDCKII-hMDR1 cells were grown in 175 cm^2 culture flasks using DMEM with 10% fetal bovine serum, 1% L-glutamine and 50 U/mL penicillin, 50 mg/mL streptomycin at 37ºC in 5% CO_2 atmosphere. Cells were split twice a week at 70-80% confluency in a ratio of 1:40, after at least 2 washes in PBS and being trypsinized with 0.25% trypsin/EDTA. All transport assays were done with cells from passages 30 to 55. Cells were kept at 37°C in 5% CO_2.

Single substrate efflux assay. Cells were seeded in 12 well Costar-Transwell plates with polycarbonate membrane inserts at a density of 175,000 cells per insert and grown for four days in culture medium. Cells were given fresh media 1 day after seeding. On the day of the

experiment, culture media was removed and cells were pre-incubated for 30 minutes with either transport media alone or transport media with 2 uM GF120918, an inhibitor of P-gp. Efflux of amprenavir, digoxin, loperamide and quinidine across the confluent monolayer of cells was measured in both directions, i.e. apical to basolateral (A>B) and basolateral to apical (B>A) in the presence and absence of GF120918. ^{3}H-amprenavir, ^{3}H-digoxin, ^{3}H-loperamide or ^{3}H-quinidine (0.5 mCi/mL) was added to each respective substrate concentration to allow quantitation of efflux from donor to receiver chambers. Lucifer yellow (100uM) was added to the donor chamber to monitor integrity of the confluent cell monolayer.

Samples (25 uL) were taken over a period of 4 or 6 hours, as shown, from both donor and receiver chambers into 96-well Lumaplates, dried overnight and the radioactivity counted by TopCount Model 9912 (Perkin Elmer, USA). The initial concentration measurement was taken at 6 min after the addition of substrate in the first well (Tran et al., 2005) and subsequent measurements taken at multiple time points up to 6 hours for all experiments (Tran et al., 2005). After taking each aliquot, the Transwell plates were placed in a shaker at a speed of 30 rpm, at 37ºC in 5% CO_2. Fluorescence of lucifer yellow (Ex max = 438nm, Em max = 530nm) was measured at time zero from aliquots taken directly from the vials and compared to samples aliquoted at the end of the experiment from both the basolateral and apical chambers; the fluorescence was analyzed using a SpectraMax microplate reader. Passive permeability of Lucifer yellow was always <10 nm/s over the entire experiment.

Cell stability and substrate metabolism. The cells do not lose any capacity for drug transport over 6 hour incubations (Tran et al., 2005; Acharya et al., 2006), implying that cellular ATP levels remain adequate for full P-gp function throughout the experiment. We showed previously that the stability of the cell monolayer and plasma membrane with respect to passive and active

transport was not affected by the prolonged exposure times to amprenavir for at least 6 hr (data not shown; Tran et al., 2005). It was also shown that metabolism or decomposition was insignificant for amprenavir, quinidine and loperamide on this time scale using radio-HPLC (data not shown; Tran et al., 2005).

Inhibition studies. Cells were seeded and fed as described above. On the day of the experiment culture medium was removed by aspiration. The cells were then preincubated with the inhibitor/substrate drugs in both chambers for 30 min. During the preincubation, half the wells received inhibitor solution without GF120918 (to study active transport) and the other half received inhibitor solution with GF120918 (to study passive transport). After 30 minutes, the preincubation solutions were removed by aspiration and the labeled substrate was added to the donor chamber, while refilling fresh inhibitor drug solution in both chambers, again one half without GF120918 and the other half with it.

Digoxin cell concentration exclusion assay. Cells were seeded and fed as described above. On the day of the experiment, culture medium was removed by aspiration. The cells were then pre-incubated for 30 minutes with transport media (TM), TM + quinidine (20uM), TM + GF120918 (2uM), or TM + quinidine (20uM) +GF120918 (2uM) in both chambers. The same protocol was repeated with an additional 1uM benzbromarone. All these pre-incubation conditions were in triplicates. Pre-incubation solutions were then removed by aspiration. Donor and receiver solutions contain the radiolabelled substrate digoxin (5uM), in addition to the respective preincubation condition. Basolateral and apical chambers were filled with donor and receiver solutions respectively. Transport from B>A was measured over 4 hours. Since the same concentration of digoxin was used on both sides, a flat curve showing steady state was obtained. At the 4th hour, all solutions were removed. Both chambers were washed 3 times with cold

transport media containing 2uM GF120918. The polycarbonate membrane inserts with the cells

were carefully cut out and radioactivity associated to the cells on the membrane was counted by

liquid scintillation.

Numerical integrations. We used the stiffest integrator in MATLAB, ode23s, with absolute

and relative tolerances set to 10^{-8}. Other MATLAB integrators, while faster, were not accurate

enough at the later times of simulations. In data fitting, all concentration curves are

simultaneously fitted, so that despite the fact that the A:B>A curve, i.e. substrate concentration in

the apical chamber when the basolateral chamber is the donor, is the most visually striking, all

curves contribute to minimizing the difference between data and simulated curves. MATLAB

fminsearch minimizes the coefficient of variation between the data and the simulated curves.

Further details can be found in Tran et al. (2005) and Bentz et al. (2005).

When the fitting included the novel basolateral and apical transporters, both Vmax and Km were

fitted independently using Eq. (3) in the mass action kinetic model for transport (Tran et al.,

2005; Acharya et al., 2006). For the best fits, the Vmax and Km values did not converge, but

their ratio was constant for all concentrations of loperamide (Vmax/Km=100 s^{-1}) and digoxin

(Vmax/Km=30 s^{-1}), Table 1. For loperamide, this value was the average of the best fits for a

concentration range 0.012-10 uM, i.e. 3 orders of magnitude, suggesting that a single transporter

is responsible for the increased flux.

Statistical Analysis. For the digoxin and loperamide data, we sought statistical validation for the

proposed basolateral (BT) and apical (AT) transporters. To compare the predictions by the

kinetic model and actual measured amounts of digoxin in apical and basal compartments over

time , we sought to evaluate four hypotheses: that predictions from adequate models would 1) be

highly correlated with empirical measurements; 2) have small root-mean-square (RMS)

prediction errors; 3) be linearly related to empirical measurements; and 4) a slope of one for the

regression of empirical data on the predictions. Regressions were performed using singular

value decomposition (Press et al. 1992). Refinement of predictions by allowing curvilinear

regressions was measured by the contribution of second order terms to minimizing prediction

errors (Rao 1998, Quinn and Keough 2002). Regression slopes were compared to unity using t-

tests comparing the estimated slopes to the hypothetical values (Sokal and Rohlf 1995, Rao

1998).

Because amounts of digoxin remaining in the basal compartment or transported to the apical

compartment were measured, sequential measurements were potentially autocorrelated and

hence, not independent, violating an assumption of regression analyses. To circumvent this, we

performed auto correlation analyses that showed that with lag times of 2-3 hours, autocorrelation

r^2 fell to <0.01 with p > 0.70. Hence, values were independent after this time lag. All analyses

reported here used sequential time points every three hours.

Loperamide trials were shorter than the stitched digoxin trials (6 vs 30 h), but transport

experiments were run for several initial concentrations of loperamide. Assuming that parameters

remained constant at all loperamide concentrations, allowed us to construct an analysis

analogous to a multiple linear regression analysis treating each transporter (P-gp-based transport,

basolateral transport by BT and apical transport by AT) as a new predictor using one degree of

freedom. The need to add further transporters to a minimal model could be tested analogously to

the need to add new predictors in a multiple linear regression model, testing the improvement of

the prediction via the decrease in the residual error of the prediction versus measurement

regression (Rao 1998, Quinn and Keough 2002). Because adding a new transporter yielded an

entirely new simulation and an entirely new prediction, this approach technically does violate

one of the assumptions of the linear analysis, i.e. independence of the transporters. Therefore,

the probability estimates must be regarded as approximate.

Mass Action Kinetic Model

Figure 1 is a cartoon of a confluent cell monolayer, featuring the polarized MDCKII-hMDR1 cells, where the basolateral membrane is attached to the polycarbonate filters and P-gp (upward arrows) expressed on the apical surface. The apical and basolateral chambers are kept separate by the tight junctions. Active transport by P-gp occurs vectorially, with substrate binding to a site on P-gp within the apical membrane inner monolayer and with efflux into the apical chamber (Loo and Clarke, 2005; Lugo and Sharom, 2005).

With the confluent cell monolayer system, we measure the concentration of substrate in the apical chamber, denoted C_A, and the basolateral chamber, denoted C_B. However, the concentration of substrate in the cytosol, denoted C_C, and in the inner plasma membrane in contact with the P-gp binding site, denoted C_{PC}, cannot be measured rigorously in real time. These internal concentrations are variables of the mass action model and fitted by elementary rate constants for well-defined kinetic barriers, according to the measured values of C_B and C_A over time (Tran et al., 2005; Acharya et al., 2006).

The simplest Michaelis-Menten mass action reaction to model P-gp is:

$$T_0 + C_{PC} \; \underset{k_r}{\overset{k_1}{\rightleftarrows}} \; T_C \; \overset{k_2}{\longrightarrow} T_0 + C_A$$

$$(2)$$
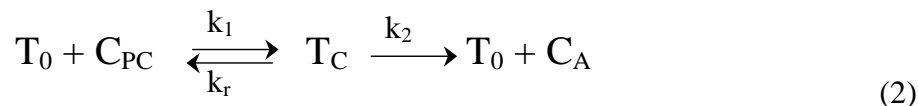
where T_0 is the empty transporter, C_{PC} the substrate in the apical membrane inner monolayer, T_C is the transporter bound by substrate and C_A the substrate after efflux into the apical chamber. Although P-gp has more than one efflux pathway with cooperative interactions at low probe-substrate and inhibitor-substrate concentrations, when the inhibitor concentrations are near the

inhibitor's IC50, P-gp behaves like a simple single competitive site transporter (Acharya et al.,

2006). The additional basolateral and apical transporters are modeled by Michaelis-Menten

steady-state equations

$$\frac{dC}{dt}\left(\text{Transporter}\right)=\frac{V_{max}\left[C\right]}{K_M+\left[C\right]}\xrightarrow{K_M>>\left[C_{PC}\right]}\frac{V_{max}}{K_M}\left[C\right]$$

(3)

This is a compromise between rigor and flexibility, since this model can roughly assess whether

there is a kinetically significant binding step to the transporter prior to influx into the cell,

without having to fit real binding constants. For each transporter, both Vmax and Km are used

to fit the data, but we have found, thus far, that only their ratio Vmax/Km (s^{-1}) was constant.

From Eq. (3), this would imply that the Km of the transporter is much larger than the substrate

concentration in the cytosol. For this modeling, we have assumed that the unknown transporters

are facilitated or bidirectional transporters, i.e. they support transport in both directions. This

was not a strong assumption, since substrate flux was mostly unidirectional import during these

experiments. Once the transporters are identified, more rigorous modeling can be applied.

For many substrates, including those studied here, passive permeability is a significant fraction

of total transport and is quantitatively analyzed separately using the P-gp inhibitor, GF120918

(Hyafil et al., 1993; Tran et al., 2005; Acharya et al., 2006). Our operational definition of

passive permeability is +GF120918, which completely inhibits P-gp and some other transporters,

both known and novel. For transporters that are not inhibited by GF120918, their transport

would be accounted for as part of the passive permeability component, regardless of their actual

mechanism of transport. The other part of the passive permeability is the passive diffusion

through the lipid bilayers of both membranes and through the tight junctions.   While the relative

contribution for each "passive" pathway is not known, that information is not essential for our

analysis of P-gp function. What is essential is that the passive permeability is accounted for as

accurately as possible, so that we can accurately measure how much of the total transport, -

GF120918, is due to P-gp and any GF120918 sensitive transporters (Tran et al., 2005).

We have fitted the drug-independent elementary kinetic rate constants of P-gp, i.e. the density of

efflux active P-gp in the apical membrane and the drug-P-gp association rate constant, using

drugs which have no other transporters in this cell line, i.e. amprenavir and quinidine (Tran et al.,

2005; Acharya et al., 2006). Thus, it is possible now to fit the kinetic parameters of these novel

transporters for digoxin and loperamide independently, as shown below.

Results

The kinetic parameters for P-gp transport published in Acharya et al. (2006) assumed that P-gp was the sole transporter. This model worked very well for amprenavir and quinidine. However, the "P-gp alone" model gave adequate fits for loperamide only with concentrations above 3uM (Tran et al., 2005; Acharya et al., 2006). At lower concentrations, more loperamide efflux was observed than could be fitted assuming the passive permeability coefficients fitted +GF120918 and the P-gp kinetic parameters fitted at high (≥3 uM) loperamide concentrations.

The loperamide data has been fitted again, now allowing a basolateral transporter, modeled by the Michaelis-Menten equation, Eq. (3). Both B>A and A>B transport data was used to find the consensus value of Vmax/Km. Here, for economy, we will only show the data and fits for the B>A transport of loperamide across MDCKII-hMDR1 monolayers. The A>B transport data fitted just as well.

Figure 2 shows the concentration of loperamide over time in each chamber and the fits for three of the eight loperamide concentrations we have examined, from 12 nM to 30 uM. The B:B>A and A:B>A curves denote the concentration of drug in the basolateral and apical chambers when the basolateral chamber was the donor, i.e. transport runs B>A. Data are shown by open squares (□) when the receiver apical chamber is sampled and by open circles (○) when the donor basolateral chamber is sampled. All data points represent triplicate measurements at each time point with the corresponding standard deviation. With the best fits, the Vmax and Km values did not converge, but their ratio was constant for all concentrations of loperamide below 30 uM, where P-gp saturated and contributes little to total transport. Vmax/Km=100±20 s^{-1}, Table 1, was the average of the best fits for loperamide concentrations from 0.012-10 uM, i.e. 3 orders of

magnitude, suggesting that a single transporter is responsible for the increased basolateral flux.

The fits are shown by a dotted line (**…**) for P-gp alone (Acharya et al., 2006) and a solid line (—)

when the basolateral facilitated transporter, denoted BT, is added using Eq. (3). In addition, all

curves contain the predicted passive efflux, +GF120918.

Fig. (2A) shows that with 0.03 uM loperamide there is a substantial underestimate of the data for

P-gp alone. With the added basolateral transporter the data fitted very well. **Fig. (2B)** shows

that with 1 uM loperamide, the two models are starting to converge, but the basolateral

transporter is clearly needed to fit the data. **Fig. (2C)** shows that with 10 uM loperamide, the

two models have converged substantially at early times, since the P-gp is nearly saturated and

most transport is through passive permeability. However, after 3 hours, the data still is fitted

somewhat better with the basolateral transporter. This is because the basolateral transporter

causes the system to need a lower apical chamber concentration and reach its true steady-state

faster. The P-gp alone simulation now overestimates the data, due to the different binding

constants needed to best fit the data without the basolateral transporter.

While the fits looked good, we wanted to quantitate their statistical significance. We compared

predictions separately for apical and basolateral compartments. In each case, predictions were

significantly improved by adding the basolateral transporter, BT, to the model with only the P-gp

transporter ($p < 5 \times 10^{-7}$). For neither the apical nor the basolateral compartment did adding an

apical transporter, AT, to the P-gp+BT model further improve the predicted concentrations of

loperamide ($p > 0.7$).

We also fitted the transport data of loperamide in the A>B direction. The fits were just as good

(data not shown). This suggests that the basolateral transporter is bidirectional, as it was

modeled.

Figure 3 shows the B>A transport of 1uM digoxin across the MDCKII-MDR1 confluent cell

monolayers. **Fig. (3A)** shows that for the first 6 hours the concentrations change roughly linearly

with time, yielding no "fittable" data. The approach to the true steady-state is required to fit the

kinetic parameters. When the cells were incubated for an extended period of time (>12 hrs), the

transport curves showed toxic effects, e.g. Lucifer yellow leakage or an A:B>A curve first

increasing and then decreasing (data not shown).

To extend the time of the experiment we constructed a data stitching experiment. **Fig. (3B)**

illustrates this construction. Once the concentrations of digoxin in the apical and basolateral

chambers at the 6th hour are known, the next experiment begins with these initial concentrations

of digoxin in the appropriate chambers. Using this approach, data is collected for consecutive

stretches of 6 hours and stitched together to create a time course up to 30 hours. The only

artifact in stitching is that for the next experiment the cytosol is initially empty of substrate,

which it would not be at the end of the prior experiment. However, since the volume of the

confluent cell monolayer cytosol is very small, the cells will fill within the first few minutes of

substrate addition, which is insignificant on the time-scale of these experiments (Acharya et al.,

2006).

The kinetic fits for the digoxin concentration time curve are shown in **Fig. (3C)**. The fits are

shown by a dotted line (**…**) for P-gp alone (Acharya et al., 2006), a solid line (—) when the

basolateral facilitated transporter, denoted BT, is added and a dashed line (_ _ _) when the

basolateral facilitated transporter and the apical facilitated transporter, denoted AT, are added

using Eq. (3). In addition, all curves contain the predicted passive efflux, +GF120918. The "P-

gp alone" model underestimates transport by at least 50% at all times. Adding a basolateral

transporter yields a good fit up to 12 hours when Vmax/Km=30s^{-1} and the parameters given in

Table 1. As mentioned about Vmax and Km were fitted independently, but only their ratio was

constant. However, beyond 12 hrs it predicts too much transport, well away from the standard

deviation of the data. Addition of an apical facilitated transporter with a Vmax/Km=2s^{-1} for

digoxin, in addition to P-gp and the basolateral transporter, yields a lower true steady-state

concentration for digoxin in the apical chamber and a good fit to the data.

To estimate the statistical significance of these fits, we compared model predictions to

measurements separately for apical and basolateral compartments. In all cases, model

predictions were highly correlated with measured amounts of digoxin in each compartment ($r^2 >$

0.90 for linear regressions). Correlations increased and RMS prediction errors decreased, in

general, when a basal transporter, BT, and then an apical transporter, AT, were added to the

models ($r^2 > 0.995$, RMS error < 0.03 for full models), Adding an apical transporter to the P-

gp+BT model neither increased the correlation nor decreased the prediction error for the loss of

digoxin from the basolateral chamber.

Regressing measured basolateral compartment digoxin data versus model predictions yielded

slopes significantly greater than 1.0 for the P-gp alone model (slope = 1.86, p < 0.01). Both the

P-gp+BT model and the P-gp+BT+AT model yielded virtually indistinguishable prediction with

slopes (0.974 and 0.984 respectively) not different from 1.0 (p > 0.05). Regressions of apical

compartment digoxin on predictions gave slopes of 1.58, 0.822, and 0.966 for the P-gp alone

model, P-gp+BT model, and P-gp+BT+AT model respectively. Only the P-gp+BT+AT model slope was indistinguishable from 1.0 at p = 0.05.

Analyses of curvi-linearity of relationships gave similar results. For basal compartment digoxin, the P-gp alone model regression was strongly curved (p < 0.01), but the other two models had no significant curvature (p > 0.05) to the regressions. For apical compartment digoxin, both the P-gp and P-gp+BT model regressions were strongly curved (p < 0.0001). The P-gp+BT+AT model, regression was significantly curved (p=0.01) but with a curvature so small that it did not affect the biological predictions.

An attempt was made to identify these canine kidney transporters involved with digoxin and loperamide transport. By preincubating cells with a "high" concentration of a substrate/inhibitor for the basolateral transporter, the transport of digoxin should decrease to the levels predicted by the P-gp efflux alone curves (e.g. a 50% reduction in digoxin transport). This makes the kinetic analysis a very sensitive instrument for determining substrates or inhibitors of the basolateral transporter. Discovering a substrate/inhibitor of the apical digoxin transporter would be more difficult, given its smaller effect on total transport.

Inhibition studies were completed with a variety of prototypical substrates or inhibitors for OAT, OATP, OCT and MRP transporters (Table 2). The compounds in Table 2 were selected because they cover a broad range of possibilities for known transporters on the basolateral or apical membranes of human and mouse kidney cells. To evaluate whether these compounds have any effect on loperamide or digoxin transport, we used concentrations at or higher than the maximum concentration used for the experiments in the respective papers. Clearly the human isoform of a

particular transporter could have a substrate or inhibitor not shared by its canine isoform. So this strategy need not succeed, but it is certainly the obvious first step.

Except for loperamide, incubations with the substrates/inhibitors failed to inhibit digoxin transport within 3hrs, B>A or A>B, the canine transporters do not interact with these substrates/inhibitors. The inhibition of digoxin transport by loperamide, and *vice versa*, certainly involves P-gp, but to determine whether they share a single basolateral transporter will need a protocol for assaying digoxin transport kinetic parameters more practical than the cumbersome "stitching" approach used here.

We did find that 100uM and 200uM benzbromarone inhibited 1uM digoxin transport in the B>A direction by 20% and 50% respectively (data not shown), but these concentrations also showed toxic effects on the cells, e.g. the transport curves stopped abruptly after a few hours and the cell monolayer became leaky. These results led us to perform the cell concentration exclusion assay using 1uM benzbromarone with the aim to find out if it actually caused less accumulation of digoxin in the cells. The amount of radioactivity from digoxin associated with the cells was measured in the presence and absence of benzbromarone. Presumably if benzbromarone inhibits the basolateral and/or apical transporter/s, then less digoxin would be accumulated within the cells.

Figure 4 shows cellular digoxin radioactivity by itself, and in the presence of quinidine (a P-gp substrate-inhibitor), GF120918 (inhibits P-gp and the additional basolateral and apical transporters) and benzbromarone. Digoxin, quinidine, benzbromarone and GF120918 are abbreviated as DGX, QND, BZB and 918 respectively. In the presence of 20uM quinidine, P-gp is relatively saturated (Acharya et al., 2006) and there is more digoxin present within the cells

compared to digoxin alone. In the presence of 2uM GF120918, P-gp and the additional

transporters are completely inactive and there is even more digoxin present within the cells, due

to the lack of P-gp efflux of digoxin. In contrast, in presence of 1uM benzbromarone there is

significantly less digoxin accumulation, suggesting inhibition of a basolateral and/or apical

uptake transporter/s, while P-gp could actively efflux digoxin.

Surprisingly, 1uM benzbromarone had no effect on digoxin transport. With 1uM benzbromarone

the monolayer was non-leaky to 4 hours, i.e. the total flux of lucifer yellow remained <10nm/s.

Therefore 1uM benzbromarone did not have a toxic effect on the cells. There is no significant

effect of 1uM benzbromarone on digoxin transport, $p < 0.05$ for both B>A and A>B directions

based on linear regression analysis (data not shown).

Discussion

The rigorous kinetic analysis of P-gp mediated transport through the confluent MDCKII-hMDR1 cell monolayer has provided a quantitative understanding of P-gp function, because the elementary rate constants so clearly define P-gp's function and the selective pressure on it (Tran et al., 2005; Acharya et al., 2006). The transport of amprenavir and quinidine across the MDCKII-hMDR1 confluent cell monolayer are quantitatively fitted by P-gp and passive permeability alone. However, for loperamide and digoxin the kinetic modeling shows other novel transporter(s) in the MDCKII cells that facilitate the passage through the basolateral membrane and for digoxin also through the apical membrane.

In Tran et al. (2005) and Acharya et al. (2006) it was noted that loperamide transport, especially at low concentrations, was being affected by another process. Adding a facilitated transporter on the basolateral membrane allows loperamide to enter the cytosol from the basolateral chamber more rapidly than predicted by the +GF120918 passive permeability coefficients, i.e. the loperamide basolateral transporter is inhibited by GF120918. We obtained good fits from 12nM to 30uM loperamide with the transporter, over 3 orders of magnitude range in concentration, Table 1. Statistical analysis supported the existence of the basolateral transporter, p<0.000001. There is no statistical evidence for an apical loperamide transporter. Since we fitted both B>A and A>B transport data for loperamide using the basolateral transporter, this suggests that it is bidirectional.

This addition to the kinetic model for loperamide has changed the estimate for loperamide's binding constant to P-gp from the apical membrane, K_C, from 4,000 M^{-1} (Acharya et al., 2006) to 20,000 M^{-1} (Table 1). The binding constant is fit primarily from A>B transport (Tran et al.,

2005) and the basolateral transporter for loperamide speeds up permeation to the basolateral chamber. Thus, a stronger binding constant to P-gp is required to fit the same A>B data.

For digoxin, the passive permeability was so slow that transport was linear with time for the first 6 hours. Without some degree of curvature, i.e. approaching steady state, fitting cannot be done. We applied a stitching method to approximate a 30-hour transport experiment. The end of one 6-hour experiment became the starting point for the next 6 hour experiment. Both a basolateral transporter and an apical transporter were needed to fit this data. We did not attempt the A>B experiment, since the transport in this direction would be much smaller, thereby making the stitching approach more problematic. We are currently working on a new protocol under which steady state should be reached faster. This will be required to determine whether digoxin and loperamide use the same basolateral transporter or not. They partially inhibit each other's transport, but we cannot yet prove whether or not this inhibition is beyond what would be predicted by inhibition of P-gp alone.

For digoxin, there is a basolateral importer and an apical importer that allows its re-entry into the cells after efflux into the apical chamber. Both were modeled as bidirectional, but only B>A data was fitted, so only import was kinetically important. Statistical analyses have shown that the basolateral transporter was required to precisely predict the amount of digoxin remaining in the basolateral compartment, $p<0.01$. Both the basolateral and apical transporters were needed to accurately predict the amount of digoxin transported to the apical compartment, $p<0.05$.

The magnitude of the increased flux of digoxin and loperamide into the cells -GF120918 proves that the basolateral transporter(s) are inhibited by GF120918. The transport of loperamide from the basolateral chamber into the cytosol is 60% due to passive permeability (+GF120918) and

40% due to the transporter (-GF120918), Table 1. The transport of digoxin from the basolateral chamber into the cytosol is 30% due to passive permeability (+GF120918) and 70% due to the basolateral transporter (-GF120918), Table 1.

On the other hand, for the digoxin transporter from the apical chamber into the cytosol, the flux is 95% due to passive permeability (+GF120918) and 5% due to the apical transporter (-GF120918). This is too small to determine whether GF120918 inhibits this transporter. This will require doing the A>B transport experiment, with an improved experimental protocol.

As a compromise between computational cost and rigor, we modeled the transporters by the Michaelis-Menten equation, with both Vmax and Km independently fitted. For all loperamide concentrations, the best fits for the basolateral transporter yielded 1-2 orders of magnitude ranges for the Km and for the Vmax, but their ratio was constant for each fit. This means that the fitting predicted a first order rate constant for this transporter, just like a passive permeability. So there was no evidence for saturation of the basolateral transporter up to 10 uM loperamide. The convergence between the P-gp alone curve and the P-gp+basolateral transporter curve is due to the saturation of P-gp at high substrate concentration.

We have tried to identify these transporters by adding prototypical substrates/inhibitors of known transporters. If we found one then the loperamide or digoxin transport curves would drop to the levels predicted by the "P-gp only" curves (Figs. 2 & 3). The change in the predicted curves would be large, making the kinetic analysis an extremely sensitive assay for discovering functional transporters in the confluent cell monolayer. While this approach is reasonable, it is always possible that the human or mouse transporters would not share a substrate/inhibitor with its canine counterpart.

None of the compounds tested in Table 2 showed simple inhibition of transport of digoxin or
loperamide during the first three hours, except loperamide and digoxin, respectively. There were
some changes noted after 3 hours, but these appeared to be related to toxicity. Since the other
transporter(s) face the basolateral or apical chambers, there is no reason why simple inhibition
would require more than 3 hours (Acharya et al., 2006).

The lack of an inhibitory effect by the P-gp substrate fexofenadine might be due to several
reasons. Fexofenadine has a very low passive permeability through Caco-2 cells (Petri et al.,
2004). We have shown that at "low" concentrations of probe-substrate and of inhibitor-
substrate, there is no inhibition of probe transport because P-gp has more than one efflux
pathway (Acharya et al., 2006). Finally, it may be that the binding constant of fexofenadine is
much smaller than that of digoxin, so a lower digoxin concentration may be needed.

A cell concentration exclusion assay was also tried, wherein the concentration of digoxin within
the confluent cell monolayer was assayed as a function of benzbromarone concentration.
Addition of benzbromarone resulted in a very significant reduction of digoxin accumulation
within the cell monolayer, as expected for a substrate/inhibitor of the basolateral digoxin
transporter. However, benzbromarone had no significant effect on digoxin B>A or A>B
transport.

The reduction in cell associated digoxin by benzbromarone is due to another mechanism besides
inhibition of the basolateral or apical transporter. The simplest hypothesis is that benzbromarone
reduces the cell's cytosolic volume, so less digoxin can accumulate. This would have no
predicted change in transport of digoxin, since the kinetic model predicts that nearly all of it
diffuses along the inner plasma membrane (Tran et al., 2005). This suggests that cell

concentration exclusion assays must be carefully controlled when used with amphipathic

compounds effluxed from a transporter whose binding sites are within the plasma membrane,

like P-gp (Lugo & Sharom, 2005).

In conclusion, we have used this rigorous kinetic analysis to detect the presence of novel

transporters of loperamide and digoxin in the basolateral membrane of this cell line, as well as a

digoxin transporter in the apical membrane. Based on the current findings, one could question

whether digoxin and loperamide are robust substrates for screening compounds for P-gp

interactions in the MDCKII-hMDR cell line. The worst case scenario in using them would be a

'false positive' if the novel compound did indeed inhibit the basolateral transporter, but not P-gp.

If a compound shows and inhibition of digoxin's efflux, a follow up experiment with amprenavir

or quinidine would identify the source of the inhibition. Quinidine and amprenavir appear to be

robust probe-substrates, as their transport across the MDCKII-hMDR1 cell monolayer depends

only upon passive permeability and P-gp. Use of another cell line, e.g. LLC-hMDRI or Caco-2,

with digoxin or loperamide does not avoid the problem, since the same kinetic analysis as shown

here is required to determine which compounds are robust P-gp probe-substrates for indivdual

cell lines.

References

Acharya P, Tran TT, Polli JW, Ayrton A, Ellens H and Bentz J (2006) P-gp expressed in a
confluent monolayer of hMDR1-MDCKII cells has more than one efflux pathway with
cooperative binding sites. *Biochemistry,* 45:15505-15519.

Bartholome K, Rius M, Letschert K, Keller D, Timmer J and Keppler D (2007) Data-Based
Mathematical Modeling of Vectorial Transport across Double-Transfected Polarized Cells.
Drug. Met. Disp. 35:1476–1481.

Bentz J, Tran TT, Polli JW, Ayrton A and Ellens H (2005) The steady-state Michaelis-Menten
analysis of P-glycoprotein mediated transport through a confluent cell monolayer cannot
predict the correct Michaelis constant Km. *Pharm Res.* 22:1667-1677.

Bentz J, Acharya P, Polli JW, Ayrton A and Ellens H (2007) Mass action kinetic analysis of
relationship between the K_I and the IC50 of P-glycoprotein substrates with the MDCKII-
hMDR1 confluent cell monolayer. *In revision*.

Dean, M, Rzhetsky, A and Allikmets, R (2001) The human ATP-binding cassette (ABC)
transporter superfamily. *Genome Res.* 11:1156–1166.

Dresser MJ, Leabman MK and Giacomini KM (2001) Transporters involved in the elimination
of drugs in the kidney: Organic anion transporters and organic cation transporters. *J. Pharm.
Sci.* 90:397-421.

Endres CJ, Hsiao P, Chung FS and Unadkat JD (2006) The role of transporters in drug
interactions. *Eur. J. Pharm. Sci.* 27:501-517.

Enomoto A and Endou H (2005) Roles of organic anion transporters (OATs) and a urate transporter (URAT1) in the pathophysiology of human disease. *Clin. Exp. Nephrol.* 9:195–205.

Harris MJ, Kagawa T, Dawson PA and Arias IM (2004) Taurocholate transport by hepatic and intestinal bile acid transporters is independent of FIC1 overexpression in Madin-Darby canine kidney cells. *J Gastroenterol Hepatol.* 19:819-25.

Horikawa M, Kato Y, Tyson CA and Sugiyama Y (2002) The potential for an interaction between MRP2 (ABCC2) and various therapeutic agents: probenecid as a candidate inhibitor of the biliary excretion of irinotecan metabolites. *Drug Metab. Pharmacokinet.* 17, 23–33.

Hyafil F, Vergely C, Du Vignaud P and Grand-Perret T (1993) In vitro and in vivo reversal of multidrug resistance by GF120918, an acridonecarboxamide derivative. *Cancer Res*. **53**:4595-602.

Ismair MG, Stanca C, Ha HR, Renner EL, Meier PJ and Kullak-Ublick GA (2003) Interactions of glycyrrhizin with organic anion transporting polypeptides of rat and human liver. *Hepatol. Res.* 26, 343–347.

Iwanga T, Kobayashi D, Hirayama M, Maeda T and Tamai I (2005) Involvement of Uric Acid transporter in increased renal clearance of the Xanthine Oxidase inhibitor Oxypurinol induced by a uricosuric agent, Benzbromarone. *Drug Metab. Disp.* 33: 1791-1795.

Juliano RL and Ling V (1976) A surface glycoprotein modulating drug permeability in Chinese hamster ovary cell mutants. *Biochim. Biophys.Acta* 455:152–162.

Kalvass JC and Pollack GM (2007) Kinetic considerations for the quantitative assessment of efflux activity and inhibition: implications for understanding and predicting the effects of efflux inhibition. *Pharm. Res.* 24:265-276.

Kikuchi R, Kusuhara H, Abe T, Endou H and Sugiyama Y (2004) Involvement of Multiple

Transporters in the Efflux of 3-Hydroxy- 3-methylglutaryl-CoA Reductase Inhibitors across

the Blood-Brain Barrier. *J.Pharm.Exp. Ther.* 311:1147-53.

Korjamo T, Kemiläinen H, Heikkinen AT and Mönkkönen J (2007) Decrease in intracellular

concentration causes the shift in Km value of efflux pump substrates. *Drug Metab Dispos.*

35:1574-1579.

Lau YY, Okochi H, Huang Y and Benet LZ (2006) Multiple transporters affect the disposition of

atorvastatin and its two active hydroxy metabolites: application of in vitro and ex situ

systems. *J. Pharmacol. Exp. Ther.* 316:762–771.

Loo TW and Clarke DM (2005) Recent Progress in Understanding the Mechanism of P-

Glycoprotein-mediated Drug Efflux. *J. Membr. Biol.* 206:173-185.

Lowes S, Cavet ME and Simmons NL (2003) Evidence for a non-MDR1 component in digoxin

secretion by human intestinal Caco-2 epithelial layers. <u>*Eur J Pharmacol.*</u> 458:49-56.

Lugo MR and Sharom FJ (2005) Interaction of LDS-751 with P-glycoprotein and mapping of the

location of the R drug binding site. *Biochemistry* 44:643-55.

Mita S, Suzuki H, Akita H, Hayashi H, Onuki R, Hofmann AF and Sugiyama Y (2006)

Inhibition of Bile Acid Transport across Na$^+$/Taurocholate Cotransporting Polypeptide

(SLC10A1) and Bile Salt Export Pump (ABCB 11)-Coexpressing LLC-PK1 Cells by

Cholestasis-Inducing Drugs. *Drug Metab Dispos.* 34: 1575-1581.

Morita N, Kusuhara H, Sekine T, Endou H and Sugiyama Y (2001) Functional characterization

of rat organic anion transporter 2 in LLC-PK1 Cells. *J.Pharm. Exp. Ther.* 298(3):1179-1184.

Morrow CS, Peklak-Scott C, Bishwokarma B, Kute TE, Smitherman PK and Townsend AJ
(2006) Multidrug resistance protein 1 (MRP1, ABCC1) mediates resistance to mitoxantrone
via glutathione-dependent drug efflux. *Mol. Pharmacol.* 69:1499-505.

Pan G and Elmquist WF (2007) Mitoxantrone permeability in MDCKII cells is influenced by
active influx transport. *Mol. Pharm.* 4:475-483.

Petri N, Tannergren C, Rungstad D and Lennernas H (2004) Transport characteristics of
fexofenadine in the Caco-2 cell model. *Pharm Res.* 21:1398-404.

Press WH, Teukolsky SA, Vettering WT and Flannery BP (1992) Numerical Recipes in C: The
Art of Scientific Computing (2nd Ed.). Cambridge University Press, Cambridge.

Quinn GP and Keough MJ (2002) Experimental Design and Data Analysis for Biologists.
Cambridge University Press, Cambridge.

Rao PV (1998) Statistical Research Methods in the Life Sciences. Duxbury Press, Pacific
Grove, CA.

Rautio J, Humphreys JE, Webster LO, Balakrishnan A, Keogh JP, Kunta JR, Serabjit-Singh CJ
and Polli JW (2006) In Vitro P-glycoprotein Inhibition Assays for Assessment of Clinical
Drug Interaction Potential of New Drug Candidates: A Recommendation for Probe-
substrates. *Drug Metab Dispos.* 34:786-792.

Sasaki M, Suzuki H, Aoki J, Ito K, Meier PJ and Sugiyama Y (2004) Prediction of *in vivo* biliary
clearance from the in vitro transcellular transport of organic anions across a double-
transfected Madin–Darby canine kidney II monolayer expressing both rat organic anion
transporting polypeptide 4 and multidrug resistance associated protein 2. *Mol. Pharmacol.*
66, 450–459.

Shitara Y, Horiea T and Sugiyama Y (2006) Transporters as a determinant of drug clearance and
tissue distribution. *Eur. J. Pharm. Sci.* **27**:425–446.

Sokal RR and Rohlf FJ (1995) Biometry. (3rd Ed) W.H. Freeman and Company, NY.

Spears KJ, Ross J, Stenhouse A, Ward CJ, Goh LB, Wolf CR, Morgan P, Ayrton A and
Friedberg TH (2005) Directional trans-epithelial transport of organic anions in porcine LLC-
PK1 cells that co-express human OATP1B1 (OATP-C) and MRP2. *Biochem. Pharmacol.* 69:
415–423.

Sugiyama D, Kusuhara H, Shitara Y, Abe T, Meier PJ and Sekine T (2001) Characterization of
the efflux transport of 17beta-estradiold-17beta-glucuronide from the brain across the blood–
brain barrier. *J. Pharmacol. Exp. Ther.* 298:316–322.

Tahara H, Kusuhara H, Maeda K, Koepsell H, Fuse E and Sugiyama Y (2006) Inhibition Of
Oat3-mediated renal uptake as a mechanism for drug-drug interaction between fexofenadine
and probenecid. *Drug Metab Dispos*. 34:743-747.

Tang F, Horie K and Borchardt RT (2002) Are MDCK cells transfected with the human MDR1
gene a good model of the human intestinal mucosa? *Pharm Res*. 19: 773-779.

Tran TT , Mittal A, Aldinger T, Polli JW, Ayrton A, Ellens H and Bentz J (2005) The
elementary mass action rate constants of P-gp transport for a confluent monolayer of
MDCKII-hMDR1 cells. *Biophys. J.* 88:715-738.

Troutman MD and Thakker DR (2003) Novel Experimental Parameters to Quantify the
Modulation of Absorptive and Secretory Transport of Substrates by P-Glycoprotein in Cell
Culture Models of Intestinal Epithelium. *Pharm. Res.* 220:1210-1224.

Vavricka SR, Montfoort JV, Ha HR, Meier PJ and Fattinger K (2002) Interactions of Rifamycin

SV and Rifampicin with organic anion uptake systems of human liver. *Hepatology*, 36:164-

172.

Figure Legends

Figure 1. Cartoon model of an MDCKII-hMDR1 confluent cell monolayer. The apical

membrane with microvilli is on top and the basolateral membrane is on the bottom, where the

cells attach to the polycarbonate insert. Passive permeability occurs in both directions. This is

measured when P-gp (open arrows) is completely inhibited by GF120918. P-gp expressed on the

apical membrane transports substrate from the inner apical monolayer into the apical chamber.

The concentration of substrate in the apical and basolateral chambers, C_A and C_B, are measured.

The concentration of substrate in the inner plasma membrane, C_{PC}, and the cytosol, C_C, are

predicted as part of the data fitting analysis. Transporters other than P-gp are known to exist in

the basolateral and apical membranes, shown by the closed double arrows, which is not meant to

suggest that they are all bidirectional.

**Figure 2. Loperamide B>A transport data in MDCKII-MDR1 cells fitted with and without

a basolateral transporter**. The concentration of loperamide over time across the MDCKII-

MDR1 cell monolayer in each chamber is shown, as a function of different initial loperamide

concentrations in the basolateral chamber. The B:B>A and A:B>A curves denote the

concentration of drug in the basolateral and apical chambers, respectively, when the basolateral

chamber was the donor, i.e. transport runs B>A. Open squares (□) show the concentration in the

apical chamber and open circles (○) show the concentration in basolateral chamber. All data

points represent triplicate measurements at each time point with the standard deviation shown by

the error bars. The fits for P-gp alone are shown by a dotted line (**...**) (Acharya et al., 2006),

while the solid line (—) shows the effect of adding a basolateral facilitated transporter, with

Vmax/Km=100s^{-1}.   All curves also contain the passive permeability (+GP120918) contribution.

(Fig 2A) Starting with 0.03 uM loperamide shows a clear underestimate of the data for P-gp

alone. **(Fig 2B)** Starting with 1 uM loperamide shows that the two models are converging, but

the curve for P-gp and the basolateral transporter is clearly superior. **(Fig 2C)** Starting with 10

uM loperamide shows that the two models have largely converged, since the P-gp is nearly

saturated and most transport is through passive permeability. Yet, the model with the basolateral

transporter remains superior A:B>A after 3 hours.

**Figure 3. Digoxin B>A transport curve is stitched together by measuring transport across
the MDCKII-MDR1 cell monolayers over consecutive 6 hour experiments. Fig. (3A)** shows

the concentration of digoxin over time in each chamber starting with 1uM initially in the

basolateral donor chamber.   The increase of digoxin concentration in the apical chamber is

linear, so fitting was not possible. **Fig. (3B)** To measure transport for a longer time course, we

constructed a "data stitching" method. Once we know the concentrations of digoxin in the apical

and basolateral chambers at the 6th hour of Fig. (3A), we start the next experiment such that the

initial concentration of digoxin in both chambers match as closely as possible. The concentration

of digoxin in the apical chamber increases over time and nearly reaches a steady state. **Fig. (3C)**

This is the final stitched data. The fits for P-gp alone are shown by a dotted line (**…**) (Acharya et

al., 2006), while the solid line (—) shows the effect of adding a basolateral facilitated

transporter, with Vmax/Km=30s^{-1}.   All curves also contain the passive permeability

(+GP120918) contribution. P-gp alone clearly underestimates transport by at least 50%. The

solid line shows the fit from adding a basolateral transporter with Vmax/Km=30s^{-1}, in addition to

P-gp. The solid line fits up to 12 hours and beyond that, it predicts more transport than we

actually measure. An apical facilitated transporter or active importer for digoxin, in addition to

P-gp, would cause the final steady state concentration for digoxin in the apical chamber to be

smaller. This is shown by the dashed line, with Vmax/Km=2s^{-1} for the additional apical

facilitator transporter. A statistical analysis of these data shows that the basolateral transporter is

significant with p<0.01 and the apical transporter is significant with p<0.05, as explained in the

text.

Figure 4. Digoxin cell concentration exclusion by benzbromarone. This figure shows

radioactivity in disintegrations per minute from radiolabeled digoxin in MDCKII-hMDR1 cells

by itself (column A), in presence of 20 uM quinidine (column B), 2 uM GF120918 (column C)

and 1 uM benzbromarone (column D). Digoxin, quinidine, benzbromarone and GF120918 are

abbreviated as DGX, QND, BZB and 918, respectively, to fit them into the figure.

Table 1. Fitted Parameter Values with Single Substrate Experiments.

Substrate	P-gp Efflux to Apical Chamber k_2 [a] (s^{-1})	P-gp Dissociation to Apical Membrane k_r [b] (s^{-1})	P-gp Binding Constant $K_C (M^{-1})$ [c] Cytosolic Dissociation Constant $K_{D,Aq}$ (M)	Partition Coefficient K_{PC} [d]	Steady State Passive Permeability Coefficients [e] (nm/sec)	Basolateral Transporter Vmax/Km (s^{-1}) [f] % Passive Transport into cytosol	Apical Transporter Vmax/Km (s^{-1}) [f] % Passive Transport into cytosol
AMP	150	2×10^6	1000 "5 uM"	200	$P_{BA}=420\pm50$ $P_{AB}=400\pm50$	0 0%	0 0%
QND	10	1×10^5	10,000 "0.1 uM"	700	$P_{BA}=500\pm100$ $P_{AB}=500\pm100$	0 0%	0 0%
LPM	1	1×10^5	20,000 "0.01 uM"	3000	$P_{BA}=350\pm80$ $P_{AB}=400\pm100$	100±20 40%	0 0%
DGX	10	ND[g]	ND[g]	ND[g]	$P_{BA}=30\pm8$ $P_{AB}=25\pm5$	30±10 70%	2±1 5%

Table 1 continued.

[a] Estimate for the efflux rate constant k_2, from P-gp into the apical chamber, given by the ratio of the fitted $k_2T(0)$ for each drug and the center of the box value of $T(0)=2x10^{-4}$ M.

[b] Estimate for the dissociation rate constant k_r, from P-gp back into the inner apical monolayer.

[c] The binding constant between P-gp and the inner apical monolayer shown is the average of the best fits (>160 for each drug concentration). Below each binding constant, we show in quotation marks the appropriate dissociation constant for each drug relative to the aqueous phase, calculated as $K_{D,Aq} =1/(K_C*$drug partition coefficient$\{PS/PE/chol\})$, the liposome mimic for the inner apical monolayer.

[d] Equilibrium drug partition coefficient to 0.1 um PS/PE/chol (1:1:1) liposomes. This lipid composition is a rough mimic for the inner apical monolayer, as described in Tran et al. (2005).

[e] Steady state passive permeability coefficients measured across the confluent cell monolayer, in the presence of the P-gp inhibitor GF120918. P_{BA} is shown above and P_{AB} is shown beneath. The values are not always symmetric.

[f] The fits for the other transporters. Both Vmax and Km were independently fitted, but only their ratio was constant. Transport is the fraction of transport into the cytosol, B>C or A>C, due to the transporter, relative to all +GF120918 passive transport.

Table 1 continued.

g   Not Determined. The mass action equations only fit the product K_C*K_{PC}, which for digoxin is ~5×10^4 M^{-1}. This is similar to

amprenavir. The partition coefficient for digoxin has not been measured, so we cannot separately estimate the binding constant,

K_C, to P-gp or the dissociation rate constant $k_r = k_1/K_C$.

Table 2. Effect of potential basolateral and/or apical transporter substrates on digoxin and loperamide transport.

Compound	Transporter [a]	Drug used (1uM)		References
		Loperamide	Digoxin	
Benzbromarone	hMRP1-6, hURAT1,	Not tested	No effect[e] with 10uM[d]	Enomoto and Endou, 2005; Iwanga et al., 2005.
Digoxin[f]	oatp1a4,4c1,1b3,1b1, roatp2, rOat-K2	moderate inhibition with 10uM DGX	NA	Dresser et al. 2001.
Fexofenadine[f]	hOAT3,roatp3,	300uM inhibits after 4hrs	No effect with 300uM	Tahara et al., 2006.
Glycyrrhizic acid	hOATP1B1,1B3, roatp1a1, 1a4, 1b2	Not tested	No effect with 200uM	Ismair et al., 2003.
Indocyanine Green	rOat2,3, r/hOATP2	Not tested	No effect with 10uM	Morita et al., 2001.
Loperamide[f]		NA [b]	Good Inhibition	
Mitoxantrone[g]	MRP1, BCRP	No effect with 25uM	No effect with 25uM	Pan and Elmquist, 2007; Morrow et al., 2006.
Ouabain	rOatK-2, roatp2, oatp4c1, 1b3	10uM inhibits after 4hrs	10uM shows biphasic curve[c]	Dresser et al., 2001.
Para-aminohippurate	m/r Oat1, hOAT1, rOat2,3	No effect with 100uM	100uM PAH inhibits after 3hrs	Dresser et al., 2001; Kikuchi et al., 2004.
Probenecid	m/r Oat1,3,4, hOAT1, rOat-K2	No effect with 200uM	No effect with 200uM	Dresser et al., 2001; Horikawa et al., 2002; Sugiyama et al., 2001.
Rifamycin[h]	rOat2, hOATP-A,C,8,1B1, 1B3	Not tested	No effect with 3uM	Dresser et al., 2001; Vavricka et al., 2002.
Taurocholic acid	Bile acid/salt transporters ASBT,BSEP,NTCP	No effect with 200uM	No effect with 200uM	Mita etal., 2006; Harris et al.,2004.
Tetra-ethyl ammonium	Many OCTs	No effect	Not tested	Dresser et al., 2001.

Table 2 continued.

[a] The compounds used here are substrates and/or inhibitors of known mammalian

transporters. Names of all human transporters (OATs, OATPs, MRPs) are in upper case.

Transporters in mice or rats are in all lower case (oatp) or start with an upper case letter

and the rest are in lower case (Oat).

[b] NA denotes not applicable.

[c] Best inhibition is seen when there is digoxin transport in presence of ouabain without

any preincubation. 30mins preincubation with ouabain produces a jump at 4 hours in two

separate experiments.

[d] 100 and 200uM benzbromarone were tested but these concentrations had toxic effects

on cells.

[e]No effect means lack of significant (>10%) inhibition by 2 hrs.

[f]Digoxin, loperamide and fexofenadine are P-gp substrates.

[g]Mitoxantrone is an inhibitor of bcrp1/ABCG2

[h]Rifampicin is a P-gp inducer.
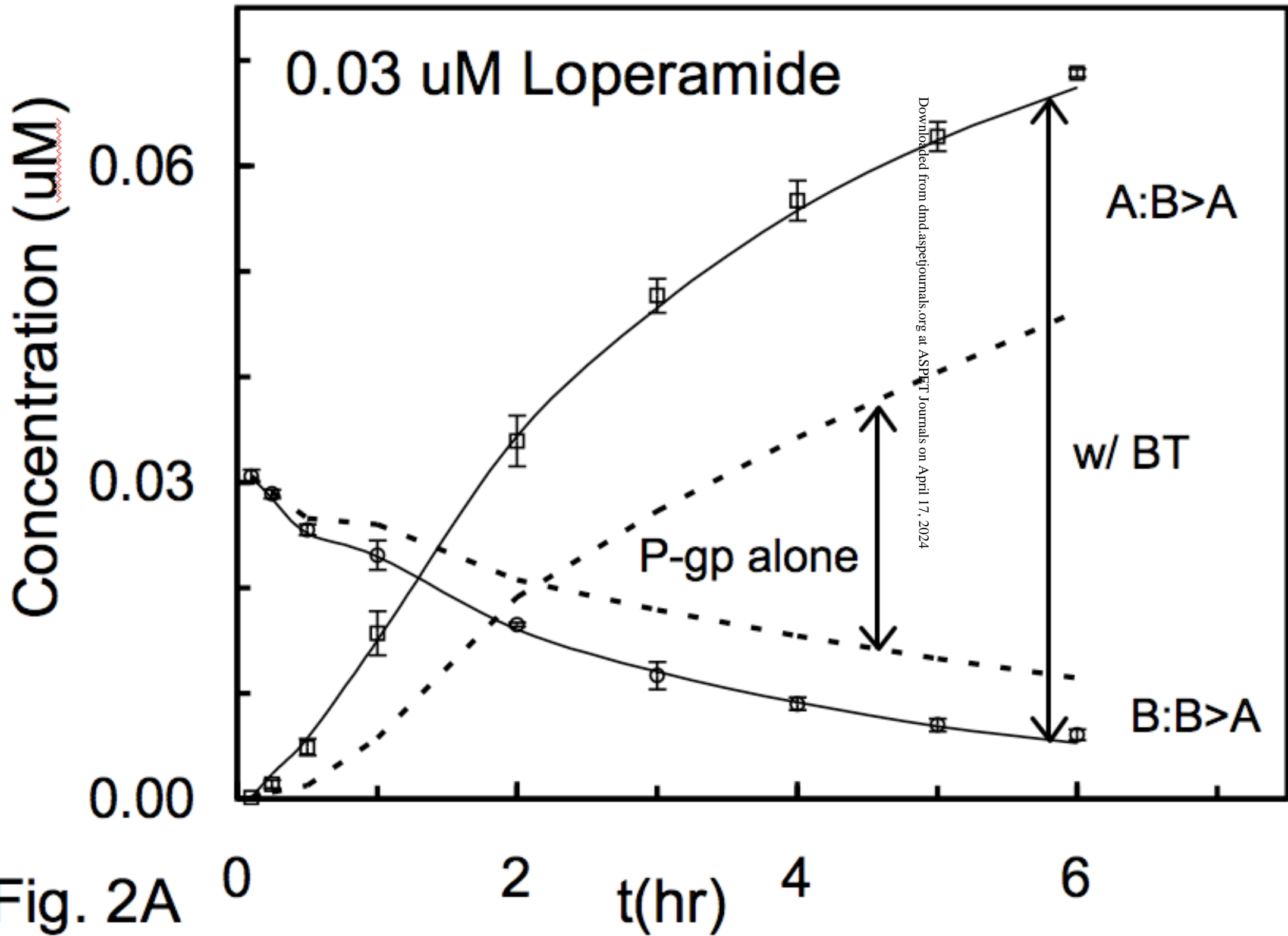
Confluent Monolayer of Polorized Cells

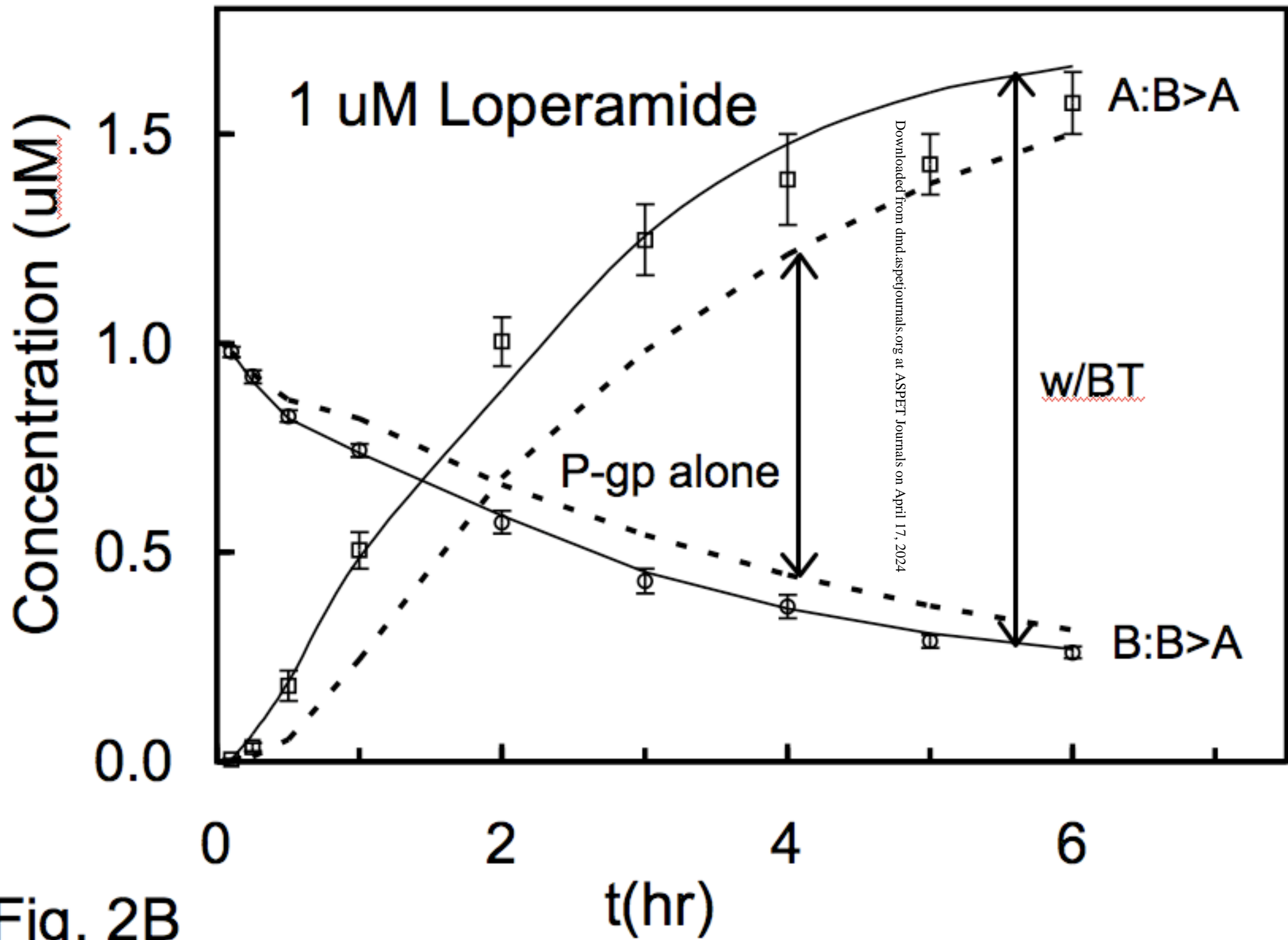Passive   Active

C_A (aqueous)

P-gp

C_{AO}

Apical

Tight
Junctions →

inner
apical
monolayer
binding
site

PC

C_C

Basolateral

Other
transporters

C_{BO}

Permeability

Fig. 1

C_B (aqueous)

Fig. 2A

0.03 uM Loperamide

A:B>A

w/ BT

P-gp alone

B:B>A

Concentration (uM)

0.06

0.03

0.00

t(hr)

0   2   4   6

Fig. 2B

1 uM Loperamide

Concentration (uM)

A:B>A

w/BT

P-gp alone

B:B>A

t(hr)

Fig. 2C

Fig. 3A

Fig. 3B

1 uM Digoxin

Expt 1
Expt 2
Expt 3
Expt 4
Expt 5

A:B>A

B:B>A

Fig. 3C

Fig. 4